Vanadium recovery from spent iron sorbent used for the treatment of mining-influenced water

Ruichi Zhang[a], Baogang Zhang[b], Tiina Leiviskä[a,*]

[a]Chemical Process Engineering, P.O. Box 4300, FIN-90014 University of Oulu, Oulu, Finland.

[b]School of Water Resources and Environment, MOE Key Laboratory of Groundwater Circulation and Environmental Evolution, China University of Geosciences (Beijing), Beijing 100083, P. R. China

E-mail: ruichi.zhang@oulu.fi (R. Zhang), baogangzhang@cugb.edu.cn (B. Zhang), tiina.leiviska@oulu.fi (T. Leiviskä)

*Corresponding author: Tiina Leiviskä

Abstract

Vanadium was recovered successfully from spent iron sorbent (ferric oxyhydroxide, CFH-12) using a two-step process including alkaline leaching and precipitation with $CaCl_2$. The spent CFH-12 was collected from a field study in which a filter system was used to remove vanadium from mining-influenced water (referred to as MIW-treated CFH-12). Fresh CFH-12 was treated with synthetic vanadium solution (SVS-treated CFH-12) to compare the recovery process with the field study. First, a full factorial design was performed to optimize the precipitation process using synthetic leaching solution. The optimal conditions were found to be two times the theoretical dosage of $CaCl_2$, a precipitation temperature of 60 °C, and a precipitation pH of 12.7. Vanadium desorption from the spent sorbents was conducted using 1 M NaOH, a contact time of 30 minutes and a CFH-12 solid-to-liquid ratio of 0.15 kg/L. The results revealed that vanadium could be efficiently precipitated from the leaching solution of MIW-treated CFH-12 and SVS-treated CFH-12. A higher dosage of $CaCl_2$ was required to recover vanadium from MIW-treated CFH-12 due to the complexity of the leaching solution, which resulted in a lower vanadium content in the product. XRD analysis showed that the

product recovered from SVS-treated CFH-12 mainly contained $Ca_5(VO_4)_3OH$ and a small amount of $CaCO_3$. TEM images revealed that the calcium vanadate hydroxide particles were round in shape, about 0.2–0.4 μm in size and formed aggregates. The product recovered from MIW-treated CFH-12 contained amorphous calcium vanadate and crystalline $Ca(OH)_2$. XPS analysis confirmed that vanadium existed as V^{5+} in all of the recovered products.

Keywords: vanadium desorption, precipitation, calcium vanadium hydroxide, full factorial design

1. Introduction

Vanadium is an important transition metal, which has been widely used in glass, textile, ceramic, steel and chemical production (Moskalyk and Alfantazi, 2003) with the majority of vanadium consumption arising from the steel industry. The addition of vanadium as an alloying element in steel manufacture can improve the hardness and wear resistance of the product (Moskalyk and Alfantazi, 2003; Perron, 2001; Zhang et al., 2011). Vanadium is the 22nd most abundant element in the Earth's crust and it can be found in over 50 different minerals including carnotite, vanadinite, roscoelite, mottramite and patronite (Perron, 2001). Although vanadium is widely distributed, the pure mineral state is never found, and the common grade in processed ore is normally less than 2% (Navarro et al., 2007). Currently, primary production of vanadium directly from mine ore and co-production from steel slags account for approximately 90% of global vanadium supply (White and Levy, 2021). However, as primary and co-production resources are limited, vanadium recovery from various secondary resources, i.e. industrial by-products, has attracted much attention.

Vanadium has been successfully recovered from oil fly ash (Chmielewski et al., 1997; Navarro et al., 2007; Vitolo et al., 2000), Bayer sludge (Gomes et al., 2017; Han et al., 2018), spent catalyst (Chen et al., 2007; Mazurek, 2013), and alloy scrap (Luo et al., 2003). The recovery procedure from these by-products has normally included leaching and precipitation/ion exchange/solvent extraction. For

example, Vitolo et al. (2001) reported vanadium recovery from oil fly ash (3.8 wt.% V) through acid leaching and oxidative precipitation using $NaClO_3$ and Na_2CO_3 after pre-treatment (burning at 850 ℃); the reported V_2O_5 content in the precipitate was 84.8 wt.%. Shao et al. (2009) recovered vanadium from desilication residue leaching solution (6 g/L V) using ammonium nitrate (50 g/L), and 92.5% of the vanadium was precipitated as ammonium metavanadate at pH 8.2. Navarro et al. (2007) extracted vanadium from oil fly ash (1.6 wt.% V) and it was reported that alkaline leaching was more selective for vanadium than acid leaching and that precipitation with ammonium salt (54 g/L, pH 5) was more efficient than solvent extraction. The results showed that more than 98% of the vanadium from the leachate could be precipitated as ammonium vanadate. Zhao et al. (2012) used CaO to recover vanadium from Bayer liquor (59 mg/L V), and the results showed that more than 83% of vanadium could be precipitated in the residue with a V_2O_5 content of 0.44% at alkaline pH.

To recover vanadium from dilute liquid streams such as mining-influenced waters, vanadium must first be concentrated before chemical precipitation. Adsorption has been regarded as a simple and efficient method for concentrating valuable metals. A variety of sorbents have been successfully developed for vanadium removal from aqueous solutions (Leiviskä, 2021); among them, commercial iron sorbents have been extensively used for vanadium removal due to their abundant functional groups, large surface area, and good availability. Different kinds of iron sorbents such as GFH/GEH 101 ($Fe(OH)_3$ and β-FeOOH), CFH-12 (FeOOH), and E-33 (α-FeOOH) have achieved sorption capacities of 22–108 mg/g in synthetic solutions (Lazaridis et al., 2003; Leiviskä et al., 2019; Naeem et al., 2007). CFH-12 and GEH 101 have also been used for the removal of vanadium from real mining waters (Zhang et al., 2021b). The vanadium sorption onto the iron oxide occurs mainly through the formation of surface complexes (Peacock and Sherman, 2004). The surface hydroxyl group bind the anionic vanadium species strongly under the optimal pH of around 3–4 (Naeem et al., 2007). In addition to surface functional groups, pore diffusion can play an important role in the vanadium sorption process and equilibrium is progressively reached (Zhang et al., 2021a). Besides

the sorbent properties, adsorption is affected by the vanadium speciation, which on the other hand is highly influenced by the conditions of the solution such as vanadium concentration, solution pH, temperature, ionic strength etc. (Wang and Sañudo Wilhelmy, 2009). It has been well demonstrated that vanadium can be desorbed from iron sorbents using alkali regeneration and the regenerated sorbent used again for vanadium sorption (Khalid et al., 2017; Leiviskä et al., 2019). In this case, the use of calcium salt for vanadium precipitation from the alkaline leaching solution would be a better choice than ammonium salt, since high acid consumption for pH adjustment can be avoided and the alkaline solution could be recirculated in the desorption stage. It should be noted that a desorption-resistant fraction in the pores could result in a slightly lower sorption capacity in the subsequent sorption cycles (Leiviskä et al., 2019), which should be taken into account in the design of the experiment in real cases. To the best of our knowledge, although many research studies have tested vanadium desorption from spent sorbents, none of them have continued vanadium recovery from those leaching solutions.

In the present study, $CaCl_2$ was used as the precipitant to recover vanadium from alkaline leaching solution. A full factorial design was first conducted to optimize the vanadium precipitation directly from the synthetic vanadium leaching solution. Based on the optimal recovery conditions, vanadium was then recovered from spent iron sorbents, which were obtained by treating CFH-12 sorbents with synthetic vanadium solution (SVS-treated CFH-12) and mining-influenced water (MIW-treated CFH-12) (collected from a field study (Zhang et al., 2021b)). The obtained products were characterized by X-ray fluorescence (XRF), X-ray diffraction (XRD), energy filtered transmission electron microscopy (EFTEM) and X-ray photoelectron spectroscopy (XPS).

2. Materials and methods

2.1 Raw materials and chemicals

Granular iron sorbent (CFH-12, ferric oxyhydroxide, Fe content 44%, particle size 1–2 mm (washed, 83%–86%) (Zhang et al., 2021b)) was purchased from Kemira Oyj (Finland). Other properties of the material can be found in Table S1. Calcium chloride dihydrate ($CaCl_2 \cdot 2H_2O$) was supplied by J.T. Baker. Stock vanadium solution was prepared by dissolving $NaVO_3$ (Sigma-Aldrich) in ultrapure Milli-Q water (Merck Millipore). Sodium hydroxide (VWR) was used as the leaching reagent. HCl (37%, Merck) was used for pH adjustment. All the chemicals used in this study were of analytical grade.

2.2 Optimization of vanadium precipitation using synthetic leaching solution

The synthetic vanadium leaching solution (SLS) was prepared by dissolving $NaVO_3$ in 1 M NaOH to reach a vanadium concentration of 420 mg/L. The concentration and pH were selected to imitate the alkaline leaching solutions from spent sorbent. Vanadium precipitation from the synthetic leaching solution was performed using a 3^3 full factorial design to optimize the precipitation conditions. The design of experiments was composed and the data were analysed using Modde 12.1 software (Umetrics). Three factors with three levels were selected (Table S2): $CaCl_2 \cdot 2H_2O$ dosage (1 time theoretical dosage (TD); 2 times TD; 3 times TD), precipitation temperature (40 °C; 60 °C; 80 °C) and precipitation pH (12.2; 12.7; 13.2). The theoretical dosage (TD) of calcium salt was estimated based on the chemical formula of $Ca_3(VO_4)_2$, which is presumed to form in the studied pH range (Li et al., 2014; Nikiforova et al., 2017). In the case of 200 mL of synthetic leaching solution (420 mg/L V), 1 time TD consumed ~0.37 g $CaCl_2 \cdot 2H_2O$. The selected pH and temperature ranges were based on previous studies using calcium in precipitation (Ding and Liu, 2011; Li et al., 2014; Zhao et al., 2012). Precipitation efficiency (%) was chosen as the response. Precipitation experiments were performed as follows: 200 mL of synthetic leaching solution was added into a 300 mL glass beaker and a certain amount of $CaCl_2$ was added according to the required dosage. The solution was agitated with a magnetic stirrer at room temperature for 30 min to ensure the homogeneity of the

123 solution. Then the pH was adjusted to the desired value using concentrated HCl and monitored with
124 a Metrohm 744 pH meter. The solution was heated up to the target temperature and then mixed for
125 five hours. Upon completion of the reaction, the solution was cooled down to room temperature and
126 the suspension was centrifuged (10 min, 2500 rpm). Next, the supernatant was sampled for residual
127 vanadium concentration analysis using the phosphorus-tungsten-vanadium spectrophotometry
128 method (UV-1800, Shimadzu) (Li, 2011). The precipitate was then filtered using vacuum filtration
129 (qualitative filter paper, 5-13 µm, VWR). The obtained product was rinsed with ultrapure Milli-Q
130 water and dried in an oven at 60 °C for 12 h. The MINEQL program (version 5.0) was used for
131 calculation of chemical speciation under the studied conditions. Carbonate concentration (in water
132 and from air) was not considered in the calculations.

133

134 2.3 Recovery of vanadium from SVS-treated CFH-12

135 SVS-treated CFH-12 was prepared by treating CFH-12 with 1000 mg/L synthetic vanadium solution
136 for 72 h to obtain the vanadium-saturated sorbent (28.5 mg/g vanadium adsorbed) and then dried in
137 the oven at 40 °C for 72 h. Vanadium desorption from CFH-12 was then performed using 1 M NaOH,
138 a contact time of 30 min and a CFH-12 solid-to-liquid ratio of 0.15 kg/L with a constant liquid volume
139 (10 mL). The concentration of leached iron from the sorbent was measured using inductively coupled
140 plasma mass spectrometry (ICP-MS) following standard method SFS-EN ISO 17294-2:2016.
141 Vanadium precipitation from the leaching solution was conducted under the optimal conditions
142 according to the results of section 3.1. The volume of the leaching solution was 50 mL (~0.55 g
143 $CaCl_2 \cdot 2H_2O$ was added (2TD)). Otherwise, the precipitation procedure was the same as described
144 above (section 2.2). The flow diagram is shown in Figure 1.

145

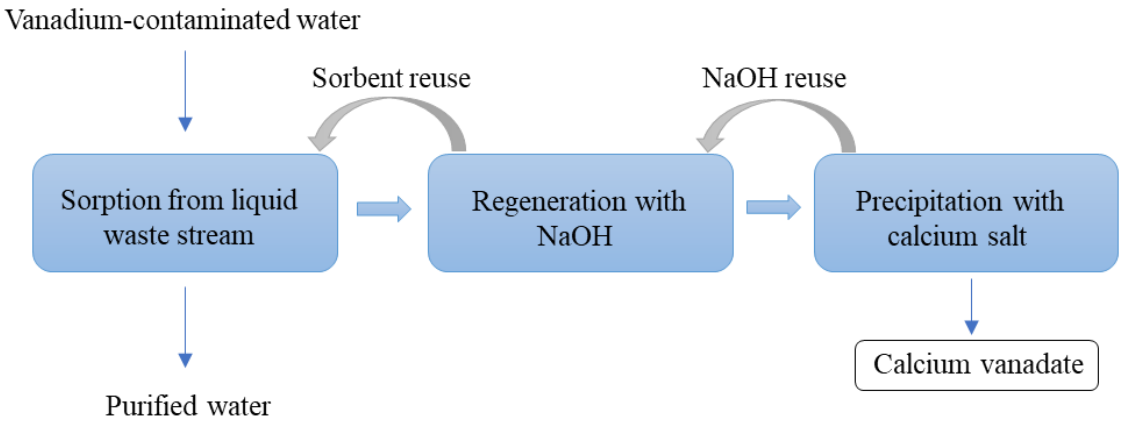

Fig. 1. Flow diagram of the vanadium recovery process.

2.4 Recovery of vanadium from MIW-treated CFH-12

MIW-treated CFH-12 was collected from a filter bed system that was used to treat real mining-influenced water at a closed mining site (Mustavaara mine, northern Finland) (Zhang et al., 2021b). The vanadium concentration varied in the mining water between 6.46 and 99.1 mg/L during the field study. The operation period was from June 10th to July 30th, 2019 (51 days). The vanadium content in the MIW-treated CFH-12 in the 10 samples collected at different points in the filter bed varied between 0.22% and 4.71% (Zhang et al., 2021b). The MIW-treated CFH-12 was first naturally dried in a laboratory and then well mixed and oven-dried at 40 °C for 72 h. Vanadium was desorbed using the same parameters as mentioned above (1 M NaOH, 30 min contact time and 0.15 kg/L CFH-12 solid-to-liquid ratio) with a constant liquid volume (10 mL). The effect of the $CaCl_2 \cdot 2H_2O$ dosage (2–8 TD (0.18–0.73 g), TD calculation based on the vanadium concentration measured by the UV method) and reaction pH (12.2 and 12.7) on precipitation efficiency was investigated. The precipitation procedure was the same as described above (section 2.3). Next, under the selected precipitation conditions, a bigger batch of the product was produced and the leaching solution before and after precipitation was sampled for detailed analysis of water quality. The pH was measured with a Metrohm 744 pH meter. A Mettler Toledo conductivity meter and a Hach 2100Q Portable turbidity

meter were used to measure the conductivity and turbidity. The chemical oxygen demand (COD) was analysed with a Hach Lange cuvette (LCK 1014). Elements were analysed using ICP-MS (SFS-EN ISO 17294-2:2016). Sulphate, chloride and fluoride were measured using ion chromatography (SFS-EN ISO 10304–1:2009). Ammonium, nitrate, nitrite and phosphate were measured with a continuous flow analyser (SFS-EN ISO 13395:1997, ISO 15923-1:2013, SFS-EN ISO 15681–2:2005).

2.5 Characterization

Products recovered from the synthetic leaching solution (SLS product) (2TD, 60 °C, pH 12.7), SVS-treated CFH-12 (SVS-CFH-12 product) (2TD, 60 °C, pH 12.7) and MIW-treated CFH-12 (MIW-CFH-12 product) (6TD, 60 °C, pH 12.7) were characterized for elemental composition using an X-ray fluorescence (XRF) spectrometer (PANalytical Axios Max). Prior to XRF analysis, the samples were ground into a fine powder and a pressed pellet was prepared using boric acid as binder under a hydraulic pressure of 10 metric tons. X-ray diffraction (XRD) analysis was performed with a Rigaku Smartlab rotating anode diffractometer using Co Kα radiation. The morphology and elemental distribution were analysed using an energy filtered transmission electron microscope (JEOL JEM-2200FS EFTEM/STEM (scanning transmission electron microscopy)) equipped with JEOL Dry SD100GV energy dispersive X-ray spectroscopy (EDS) detector. X-ray photoelectron spectroscopy (XPS) analysis was carried out using a Thermo Fisher Scientific ESCALAB 250xi with a monochromatic Al Kα source (1486.6 eV). The binding energy of the peak related to the V–O bond (530.0 eV) in the O 1s spectrum was used for calibration (Hryha et al., 2012).

3. Results and discussion

3.1 Optimization of vanadium precipitation from synthetic leaching solution

189 The effect of the $CaCl_2$ dosage, pH and temperature on vanadium precipitation efficiency was studied
190 at three different levels (Fig. 2). The precipitant dosage had a significant effect. With a higher
191 precipitant dosage (⩾2TD), over 94% of vanadium was precipitated. Lower precipitation efficiency
192 (46.2%–79.8%) was observed with 1TD $CaCl_2$ (Fig. 2). A more stable precipitation process was
193 observed at higher precipitation temperatures (60 °C and 80 °C). The precipitation process performed
194 better at pH 12.2 and 12.7 in the studied pH range.
195 The experimental data was then analysed using MODDE 12.1 (Table S3 and S4). The statistical
196 analyses suggested that, during the reaction, the precipitant dosage and reaction pH were significant
197 (*p*-value <0.05), whereas the temperature in the studied range was insignificant (*p*-value >0.05). In
198 addition, the interactions between different factors were not significant (*p*-value >0.05). The
199 precipitant dosage had a positive effect, while the reaction pH had a negative effect on the vanadium
200 precipitation efficiency in the studied range (Table S4), suggesting that the efficiency would increase
201 with an increased precipitant dosage and decreased reaction pH in the studied range.

202 Chemical speciation calculations show that calcium salt is able to precipitate vanadium by forming
203 different stable solid Ca-V compounds (Fig. 3). Below pH 2, vanadium mainly exists in a soluble
204 cationic form. In the pH range of 2.8–4.6, $H_3V_2O_7^-$ becomes the dominant species. Insoluble calcium
205 vanadate starts to form at pH values higher than 4.6. Vanadium exists as $Ca_2V_2O_7$ at pH 6.3–10.5 and
206 as $Ca_3(VO_4)_2$ at pH 10.85–13.65. However, with a further increase in pH, the vanadium takes a
207 soluble form and portlandite ($Ca(OH)_2$) started to become the principal precipitate. These results are
208 also in agreement with a previous study, in which $Ca_3(VO_4)_2$ was formed in a higher pH range (>10)
209 and, among the different Ca-V compounds, minimum vanadium concentration was reached when
210 $Ca_3(VO_4)_2$ was formed (Li et al., 2014). As reaction pH values of 12.2 and 12.7 both resulted in a
211 good precipitation efficiency, pH 12.7 is suggested when a strong alkaline leaching solution is
212 obtained, as it reduces the chemical consumption in pH adjustment. In addition, the percentage of

impurities (e.g. $Ca(OH)_2$) increases at a higher $CaCl_2$ dosage (Fig. S1, in this case with 3TD). Therefore, 2TD $CaCl_2$ was used in the next stage.

Although the statistical analyses indicated that the reaction temperature in the studied range was an insignificant factor during the precipitation process, it was observed that the precipitate formed at the reaction temperature of 40 °C sometimes resulted in a very turbid solution, especially when a lower $CaCl_2$ dosage was used and the precipitation efficiency fluctuated under the specific conditions (1TD $CaCl_2$, 40 °C, pH 13.2). This suggested that the reaction might be more efficient and stable at a higher reaction temperature. In addition, Zhao et al., (2012) have reported that a higher temperature was favourable to precipitate vanadium from Bayer liquor ($Al(OH)_4^-$ as the major component along with $SiO_2(OH)_2^{2-}$, CO_3^{2-}, VO_4^{3-}) with lime, since the side reactions could be inhibited to a certain extent. As a similar precipitation efficiency was obtained at 60 °C and 80 °C in this study, 60 °C was thus selected for further experiments with the aim of energy savings in real applications.

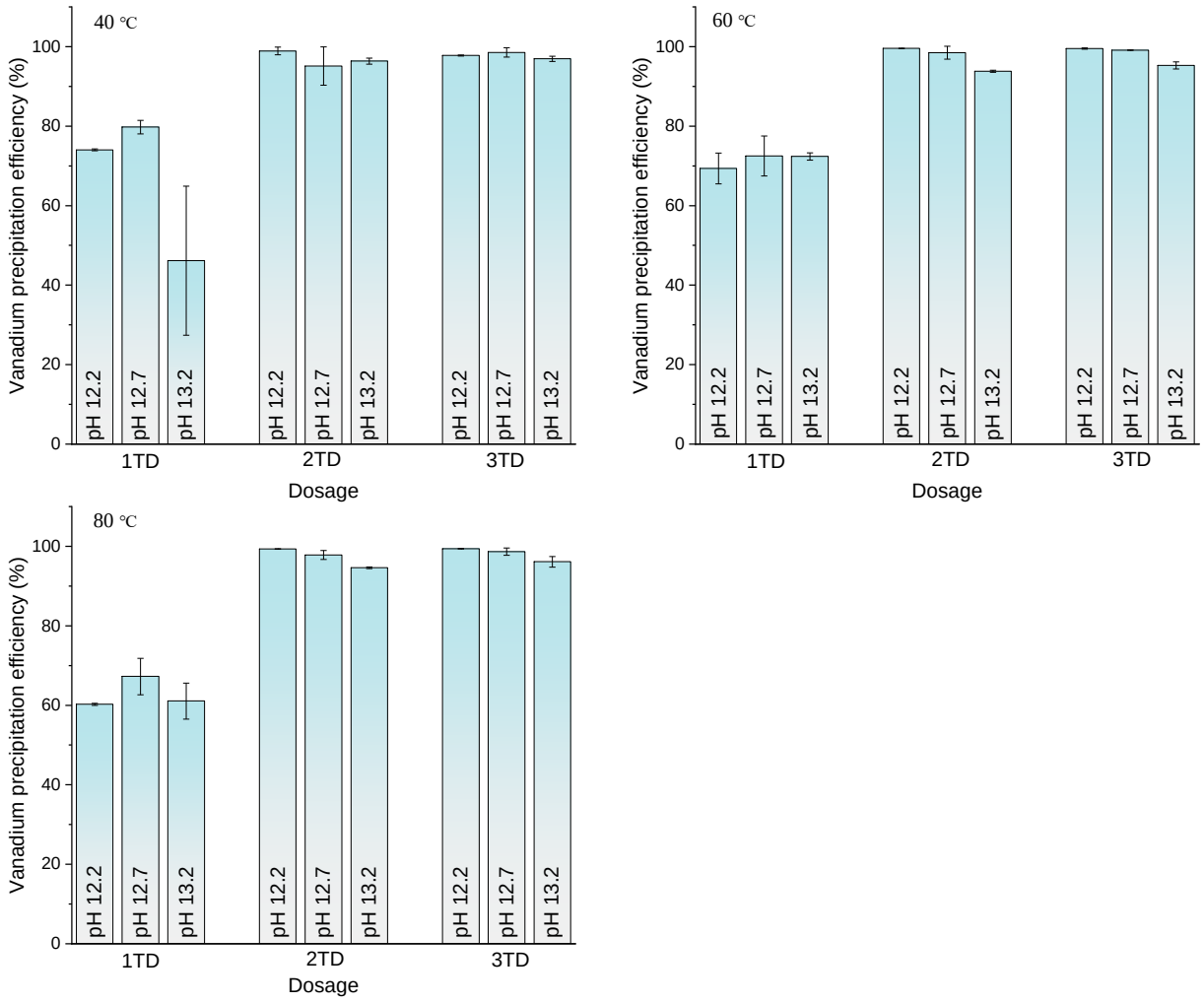

227

228 Fig. 2. Effect of precipitant dosage ($CaCl_2$), precipitation temperature and precipitation pH on
229 vanadium precipitation efficiency (error bars represent the range of two repeats, except for the 1TD
230 $CaCl_2$, 40 °C, pH 13.2 experiment, which had four repeats).

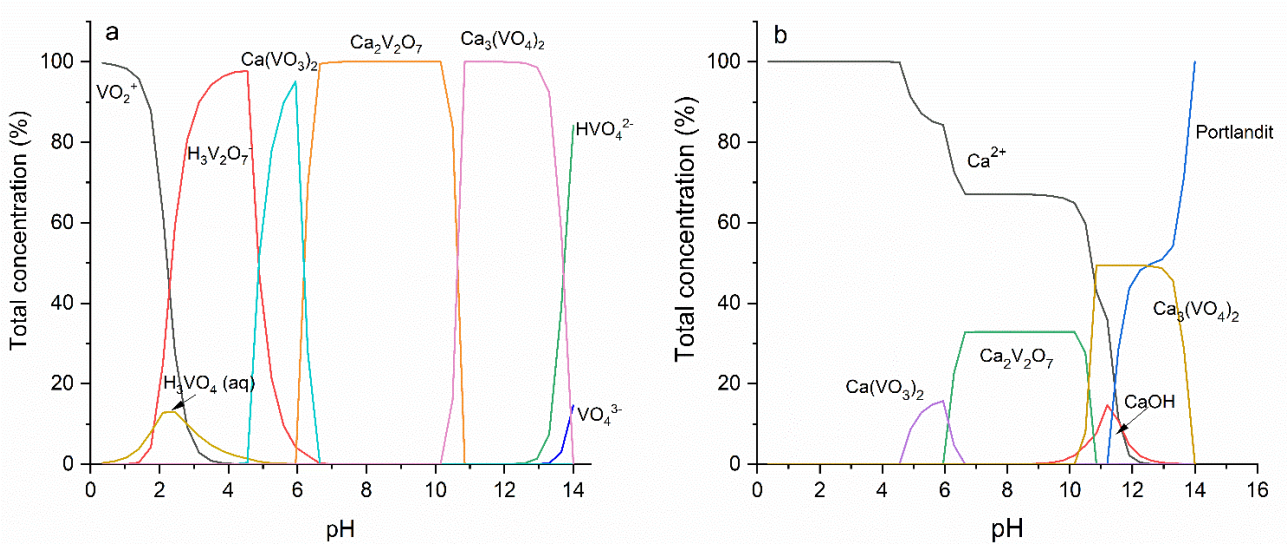

231

232 Fig. 3. Distribution diagram of (a) vanadium and (b) calcium species as a function of pH at 60 °C
233 (solution: synthetic leaching solution; vanadium concentration: 8.23 mM (420 mg/L); calcium
234 concentration: 0.025 M (1 g/L) (2TD)).

235

236 3.2 Vanadium recovery from SVS-treated CFH-12

237 Alkaline pH conditions can be used to desorb vanadium, since OH^- ions are able to replace vanadium
238 anions from the surface binding sites (Guzmán et al., 2002). The desorption of vanadium from SVS-
239 treated CFH-12 was performed first (1 M NaOH, 30 min contact time and 0.15 kg/L CFH-12 solid-
240 to-liquid). The obtained leaching solution contained 1275 mg/L V and also a high concentration of
241 sulphate (6250 mg/L). The sulphate originated from a gypsum impurity contained in the CFH-12,
242 which was reported in a previous study (Leiviskä et al., 2019). Additionally, it was observed that the
243 NaOH treatment significantly increased the surface area and pore size of the CFH-12 sorbent
244 (Leiviskä et al., 2019).

245 The precipitation experiment from the leaching solution was conducted in the optimal conditions
246 according to section 3.1 (2TD $CaCl_2$; precipitation temperature 60 °C; precipitation pH 12.7). The
247 vanadium precipitation reached 99.9% and was presumed to exist as $Ca_3(VO_4)_2$ (Fig. 3). However,
248 the overall vanadium recovery rate from SVS-treated CFH-12 was quite low, at 44.6%, (44.7%

desorption efficiency with 1 M NaOH + 99.9% precipitation efficiency) but this can be improved e.g. by increasing the concentration of the NaOH solution (Khalid et al., 2017; Leiviskä et al., 2019). Nevertheless, further optimization is still needed, for example by investigating possible iron leaching at higher NaOH concentrations, and also the effect of temperature on desorption could be studied. A negligible amount of iron (approx. 0.03%) was leached from the sorbent in this study with 1 M NaOH. Also, it is worth noting that a higher amount of acid will be needed in the precipitation stage if desorption is carried out with a more concentrated NaOH solution.

The calculated distribution of vanadium, calcium, and sulphate species is shown in Fig. 4. A similar trend was observed as the one found for the SLS product (section 3.1). In addition, sulphate existed in soluble form at the higher pH values (pH >11.9, Fig. 4c). Therefore, the leached sulphate probably did not affect vanadium precipitation in the studied pH range.

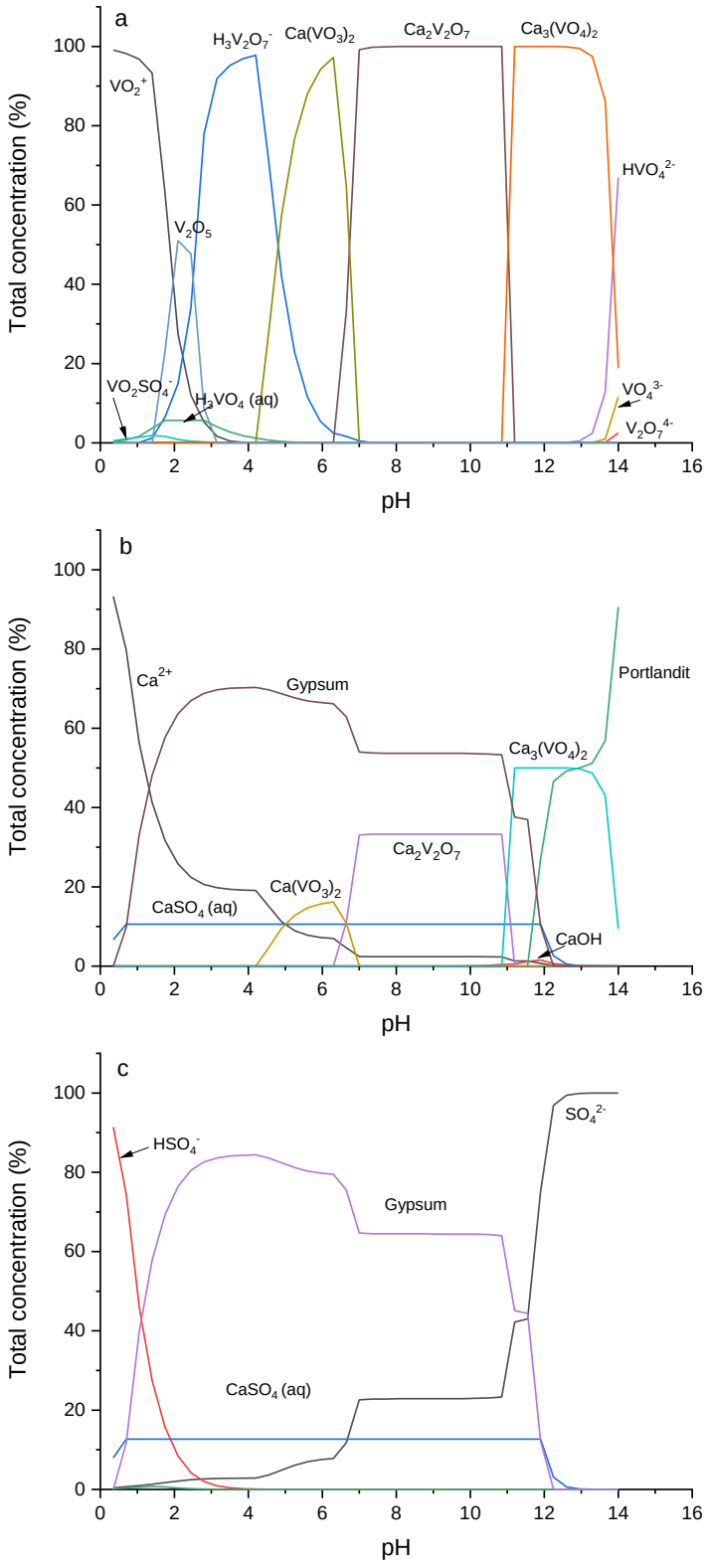

Fig. 4. Distribution diagram of (a) vanadium, (b) calcium and (c) sulphate species as a function of pH at 60 °C (solution: leaching solution from saturated iron sorbent; vanadium concentration: 25 mM

(1275 mg/L); calcium concentration: 0.075 M (3 g/L) (2TD); sulphate concentration: 0.065 M (6.25 g/L)).

3.3 Vanadium recovery from MIW-treated CFH-12 collected from the field study

A field study provided a realistic sample for this study as MIW-treated CFH-12 was used for vanadium recovery. The vanadium desorption parameters were the same as those used for the SVS-treated CFH-12 (1 M NaOH; 30 min contact time; 0.15 kg/L CFH-12 solid-to-liquid ratio). The precipitation experiment was conducted at the temperature of 60 °C with different $CaCl_2$ dosages (2TD–8TD) and reaction pH values (12.2 and 12.7). Vanadium precipitation efficiency was in the range of 33%–99% (Fig. S2). The results showed that there were no differences between pH 12.2 and 12.7 in the vanadium precipitation process. Therefore, pH 12.7 was considered as the optimal pH because less acid would be needed to adjust the pH of the leaching solution. To reach over 90% precipitation efficiency, a higher $CaCl_2$ dosage was required to recover vanadium from the MIW-treated CFH-12 than was required in the case of the SVS-treated CFH-12. For the leaching solution of MIW-treated CFH-12, vanadium precipitation efficiency was only 34% when 2TD $CaCl_2$ was used, while the efficiency improved to 81% with 4TD $CaCl_2$. The precipitation efficiency continued to increase to 97% with 6TD $CaCl_2$ and reached 98% by further increasing the dosage to 8TD. As 6TD and 8TD $CaCl_2$ resulted in almost the same precipitation efficiency, the lower dosage (6TD) was thus selected for further analyses. It is noteworthy that, although the precipitation process in the case of MIW-treated CFH-12 consumed more $CaCl_2$ compared to SVS-treated CFH-12 and increased the proportion of impurities, the purity of the recovered product normally needs to be improved through further treatment, e.g. calcination after converting it to ammonium metavanadate (Muthukumar et al., 2020; Wang et al., 2017).

The detailed water quality analysis of the MIW-treated CFH-12 leaching solution before and after precipitation (6TD $CaCl_2$; precipitation temperature 60 ℃; precipitation pH 12.7) is presented in

Table 1. The higher required calcium dosage compared to the SVS-treated CFH-12 is probably due to the complexity of the leaching solution from the MIW-treated CFH-12, as some other compounds (e.g. Al, Fe, Cu and PO_4^{3-}) from the mining effluent were also adsorbed onto the CFH-12 (Zhang et al., 2021b) and some were leached out during the desorption stage, as shown in Table 1. Besides vanadium, the leaching solution contained a considerable amount of sulphate (1700 mg/L), which was mainly due to the leaching of the gypsum impurity from the CFH-12 used (Leiviskä et al., 2017). However, the sulphate concentration was significantly lower compared to the leaching solution of the SVS-treated CFH-12 (6250 mg/L), which is probably due to the long duration of the field test, during which most of the impurities in the CFH-12 were leached out.

After precipitation, the vanadium concentration in the leaching solution significantly decreased from 370 mg/L to 23 mg/L (Table 1). The conductivity, turbidity and the concentration of other ions such as F^-, PO_4^{3-}, Al and Fe also decreased significantly in the solution after precipitation, although the original concentrations of these ions were much lower than that of vanadium. Conversely, the sulphate concentrations were at almost the same level before and after precipitation, which supported the assumption that sulphate did not affect vanadium precipitation in the studied pH range. This is in agreement with the speciation data (section 3.2), i.e. sulphate exists in soluble form (SO_4^{2-}) at high pH. It should be noted that the chloride concentration dramatically increased after precipitation, which was due to the addition of $CaCl_2$ and HCl (for pH adjustment) to the solution. Furthermore, this leaching solution was brown in colour and resulted in a light brown precipitate, which might have originated from the natural organic compounds adsorbed from the mining effluent.

Table 1. Characteristics of the leaching solution from MIW-treated CFH-12 before and after vanadium precipitation (6TD $CaCl_2$; precipitation temperature 60 ℃; precipitation pH 12.7). (N.A. = not available, chloride interferes with COD analysis).

Parameter	Unit	Leaching solution	Solution after precipitation
pH	/	13.6	11.7
Conductivity	ms/cm	116	66
Turbidity	NTU	20.6	1.2
COD	mg/L	1266	N.A.
Cl^-	mg/L	4	21000
F^-	mg/L	13	4.5
SO_4^{2-}	mg/L	1700	1600
NH_4^+	mg/L	0.44	0.4
NO_2^-	mg/L	-	0.27
NO_3^-	mg/L	-	0.13
PO_4^{3-}	mg/L	31	0.041
V	mg/L	370	23
Al	mg/L	9.9	2.5
B	mg/L	1.6	1.2
As	µg/L	61	6,9
Co	µg/L	2.9	1.8
Cr	µg/L	20	16
Cu	µg/L	68	49
Fe	µg/L	470	<50
Mn	µg/L	5	<0.4
Mo	µg/L	540	510
Ni	µg/L	23	15
Se	µg/L	15	9.5

Sn	µg/L	1.4	<1
Sr	µg/L	<2	85
U	µg/L	18	<0.2

313

314 3.4 Characterization

315 3.4.1 XRF analysis

316 The main composition of the recovered products was determined by XRF analysis (Table S5).
317 Calcium and vanadium are the main elements in all three products, whereas the percentage of
318 vanadium is higher in the SLS product (11.2%) and the SVS-CFH-12 product (11.3%) than in the
319 MIW-CFH-12 product (7.1%) due to the higher dosage of $CaCl_2$ used in the case of MIW-CFH-12.
320 In addition, a small amount of sulphur was detected in the SVS-CFH-12 and MIW-CFH-12 products
321 and was slightly higher in the SVS-CFH-12 product, which indicates that not all of the sulphur
322 remained in the leaching solution after precipitation. This result is consistent with the finding that the
323 sulphate concentration was higher in the leaching solution of SVS-treated CFH-12 than in the solution
324 of MIW-treated CFH-12 (section 3.3). Additionally, other elements such as phosphorus, silicon,
325 aluminium, chlorine etc. were also detected in minor amounts in the recovered products.

326

327 3.4.2 XRD analysis

328 The XRD profiles of the recovered products are shown in Fig. 5. In the SLS product, $CaCO_3$ and
329 $Ca(OH)_2$ were identified with certainty. The XRD pattern of the SLS product also contained some
330 unidentified peaks. Accurate identification of the Ca-V compound by XRD was not possible.
331 Different forms, for example, calcium vanadium oxide and calcium vanadium oxide hydrate, are
332 possible. The SVS-CFH-12 product contains calcium vanadium hydroxide ($Ca_5(VO_4)_3OH$) as the
333 major component, while a small amount of calcium carbonate ($CaCO_3$) can also be observed in the

recovered product (Fig. 5). The XRD results of the SLS and SVS-CFH-12 products differ from the speciation calculation, which suggested that the precipitate contained only $Ca_3(VO_4)_2$ and $Ca(OH)_2$ (section 3.2.2). However, carbonate was not considered in the modelling calculations and data for $Ca_5(VO_4)_3OH$ is not available in the database.

The vanadium in the MIW-CFH-12 product (with 6TD $CaCl_2$) exists as an amorphous phase, and the major crystalline phase observed is $Ca(OH)_2$. This can be attributed to the higher $CaCl_2$ dosage used to obtain the MIW-CFH-12 product. The XRD results indicate that, when the composition of wastewater is simple and a reasonable precipitant dosage is used, a higher purity product can be obtained compared to wastewaters with a complex composition.

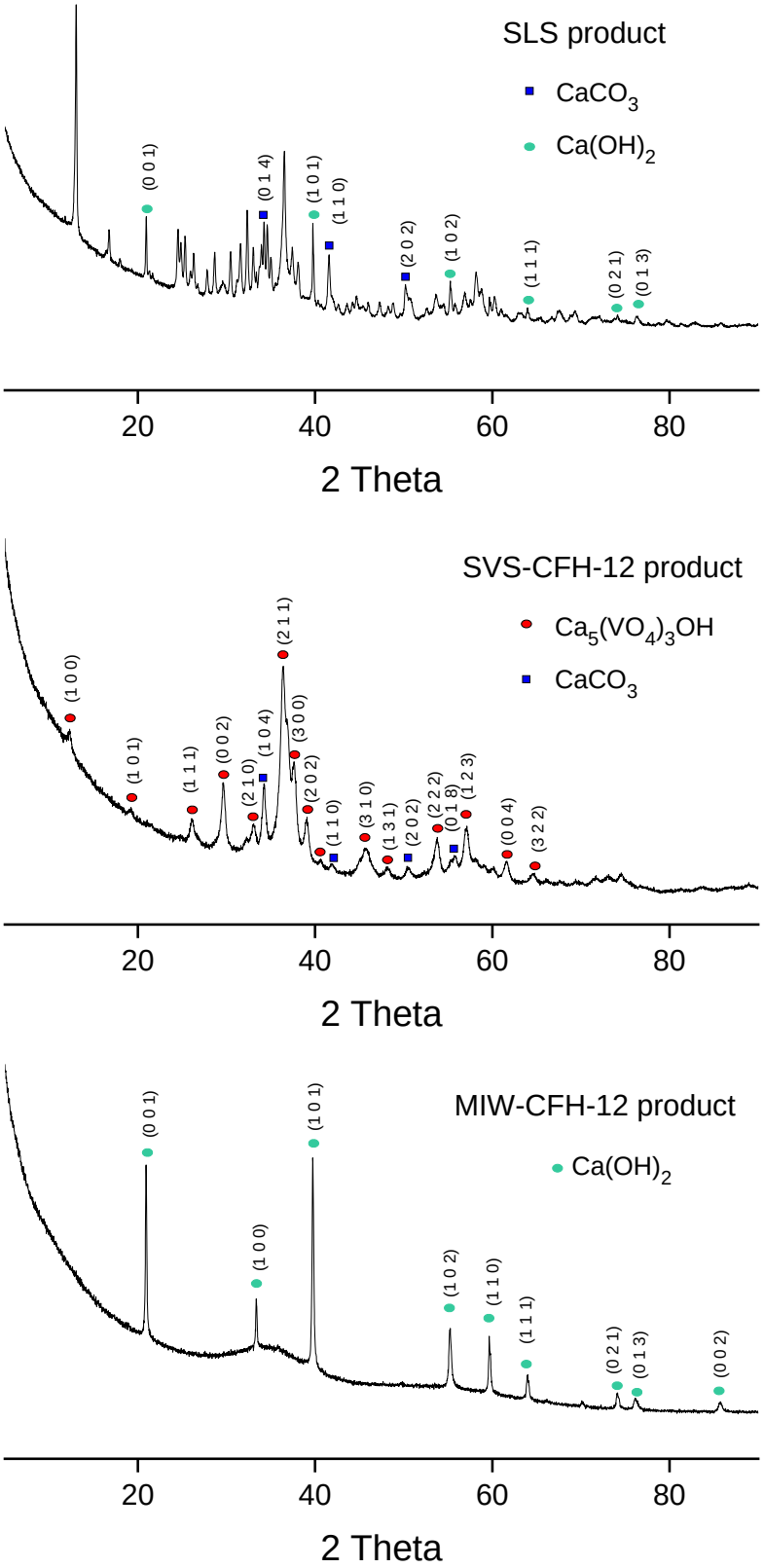

345

346 Fig. 5. XRD profiles of the recovered products.

347

3.4.3 TEM

The TEM images, the elemental maps presenting the distribution of V and Ca, and the overlay maps of Ca-V are shown in Fig. 6. Three different phases can be observed in the TEM image of the SLS product (Fig. 6a). Aggregates of round-shaped particles (0.2–0.4 µm) dominate, in which Ca and V are closely associated (Fig. 6a (4)). Then coarse rod-shaped crystals (length approx. 2–3.5 µm) can be observed, which are shown in green (Ca) in the overlay map (Fig. 6a (4)) and refer to the $CaCO_3$ crystals observed by XRD. Additionally, there are a few particles with a rod shape and a smooth surface, and these particles were suspected to be $Ca(OH)_2$.

The TEM images of the SVS-CFH-12 product show rounded calcium vanadate hydroxide particles about 0.2–0.4 µm in size, which are agglomerated to some extent (Fig. 6b); V and Ca are uniformly distributed in these particles. $CaCO_3$ particles can also be observed, as in the SLS product (displayed in green in the overlay map (Fig. 6b (4)), but to a much lesser extent. For the MIW-CFH-12 product, calcium-vanadium particles are aggregated in amorphous form and $Ca(OH)_2$ exists in crystalline form (green particles in the overlay map (Fig. 6c (4)).

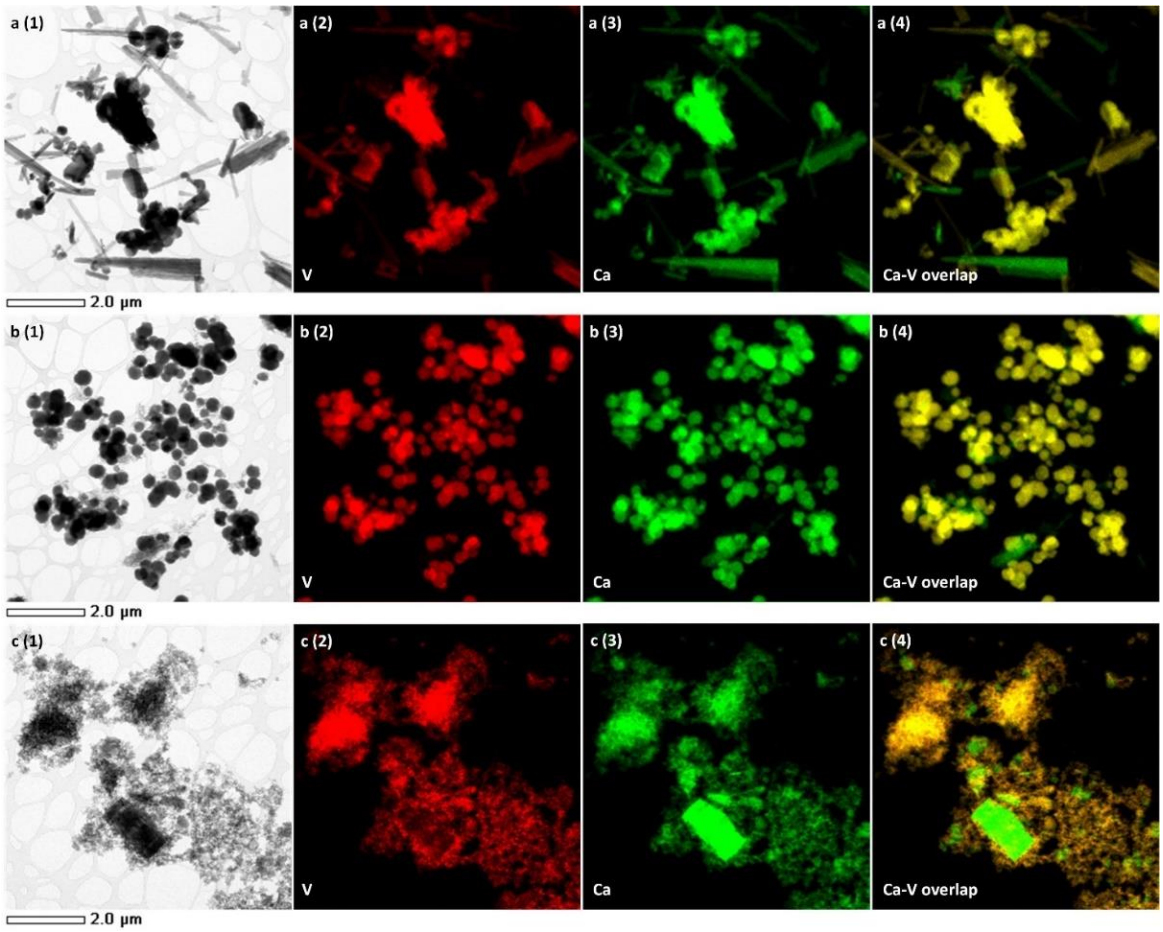

362

363 Fig. 6. TEM image and TEM element mapping of (a) SLS product (b) SVS-CFH-12 product and (c)
364 MIW-CFH-12 product.

365

366 3.4.4 XPS analysis

367 The surface elemental compositions of the recovered products was determined by XPS analysis
368 (Table S6). The weight percentage (surface) of vanadium in the SLS, SVS-CFH-12 and MIW-CFH-
369 12 products is 13.3%, 8.8% and 4.0%, respectively. The highest vanadium percentage observed in
370 the SLS product is probably due to the pure reaction system compared to the other two products. The
371 highest $CaCl_2$ dosage is the reason for the lowest vanadium content in the MIW-CFH-12 product.
372 The highest C1s proportion is observed in the MIW-CFH-12 product (17.2 wt.%), which originated
373 from the organic compounds adsorbed onto CFH-12. Fluorine was detected in all products, which

probably originates from the impurity of the reagents and sorbent. Additionally, an S 2p peak (~170 eV) was observed in the survey spectrum of the SVS-CFH-12 product, indicating that a small amount of sulphur was co-precipitated due to the high sulphate concentration (6250 mg/L) in the leaching solution of the SVS-treated CFH-12 (Yanan et al., 2020; Zhang et al., 2012). Although XRF analyses showed that the MIW-CFH-12 product would also contain a small amount of sulphur, the S 2p peak could not be observed in the survey spectrum.

All the products presented two main components in the C 1s spectra at 285.6 ± 0.3 eV and 290.0 ± 0.1 eV (Fig. 7). The component at 285.6 eV corresponds to C–C/C–H or C–O/C–N from adventitious carbon and/or adsorbed organic compounds, while the second component is related to inorganic carbonate/bicarbonate (290.0 ± 0.1 eV) (Heuer and Stubbins, 1999; Sun et al., 2006). Inorganic carbonate/bicarbonate is derived from $CaCO_3$, which was also identified by XRD in the case of the SLS and SVS-CFH-12 products. For the MIW-CFH-12 product, $CaCO_3$ was not detected by XRD, but the C1s peak at higher binding energy confirms the presence of inorganic carbonate. This might indicate that $CaCO_3$ was present in amorphous form. In addition, the peak at lower binding energy mainly originates from adsorbed organic compounds from the mining effluent.

The Ca $2p_{3/2}$ and Ca $2p_{1/2}$ peaks of all the products appear at 347.4 ± 0.2 eV and 350.9 ± 0.2 eV (full width at half maximum (FWHM) = (1.7–1.8) (Fig. 7), mainly originating from the Ca-V compound (Curelaru et al., 1981). The observed binding energy of Ca $2p_{3/2}$ is similar to the binding energy reported for Ca $2p_{3/2}$ (347.1 eV, FWHM = 1.59 eV) in hydroxylapatite $Ca_5(PO4)_3OH$ (Eighmy et al., 2000). As the products also contain small amounts of $CaCO_3$ (SLS and SVS-CFH-12 products) and $Ca(OH)_2$ (SLS and MIW-CFH-12 products), they also contribute to the Ca 2p peaks. $CaCO_3$ (the calcite polymorph) and $Ca(OH)_2$ have been reported to have a Ca $2p_{3/2}$ peak at 346.5 eV (Ni and Ratner, 2008) and 346.3 eV (Dupin et al., 2000), respectively. The V 2p spectra of all the products

present V $2p_{3/2}$ at 517.4 ± 0.1 eV and V $2p_{1/2}$ at 524.8 ± 0.1 eV (Fig. 7), suggesting that vanadium exists as V^{5+} in Ca-V compounds (Silversmit et al., 2004).

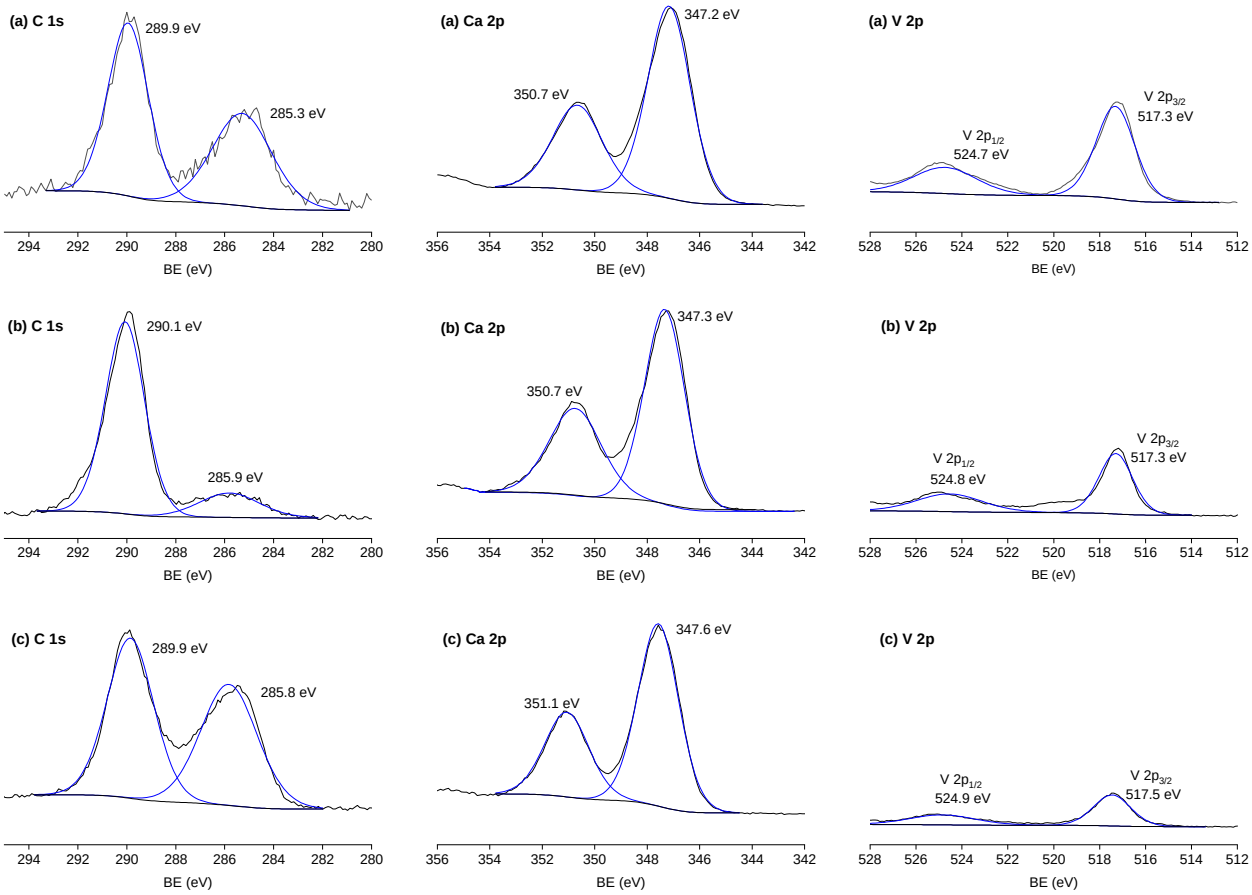

Fig. 7. C 1s, Ca 2p and V 2p high resolution XPS spectra of (a) SLS product (b) SVS-CFH-12 product and (c) MIW-CFH-12 product.

4. Conclusion

This study showed that it was possible to recover vanadium from a sorbent used to treat mining water. The recovery process consisted of vanadium desorption from the spent sorbent (1 M NaOH, 30 min contact time, 0.15 kg/L CFH-12 solid-to-liquid ratio) and vanadium precipitation with $CaCl_2$. Vanadium precipitation efficiency from the leaching solution of SVS-treated product reached >99.9% under the selected precipitation conditions (2TD $CaCl_2$, 60 °C precipitation temperature, precipitation pH 12.7), whereas for the MIW-treated CFH-12, a higher dosage of $CaCl_2$ (6TD) was required to

obtain similar precipitation efficiency (97%) at the same precipitation temperature (60 °C) and pH (12.7). XRD and TEM analysis revealed that $Ca_5(VO_4)_3OH$ existed in the SVS-CFH-12 product~~s~~, while the MIW-CFH-12 product contained amorphous calcium vanadate. Higher purity of the recovered product can be obtained from the vanadium leaching solution with a less complex matrix. The recovered product could be further purified, with a subsequent calcination after converting it to ammonium metavanadate, and used in many applications such as in the catalyst and battery industries. Moreover, after the recovery process, the circulation of leaching solution with high pH into the next vanadium desorption stage might be possible. Hence, this work provides an economical and environment-friendly way to recover vanadium from waste streams, which is important for waste management and vanadium production using alternative resources.

Acknowledgements

This work was funded by the VanProd project “Innovation for enhanced production of vanadium from waste streams in the Nordic Region”. The authors express their sincere gratitude to the European Union program Interreg Nord 2014–2020 and the Regional Council of Lapland for the financial support of this study. The authors gratefully acknowledge the support from Maa-ja vesitekniikan tuki ry and Tauno Tönning Foundation. The work was also conducted as part of the Supporting Environmental, Economic and Social Impacts of Mining Activity (KO1030 SEESIMA) research project and received financial support from the Kolarctic CBC (Cross-Border Collaboration), the European Union, Russia, Norway, Finland and Sweden. Its contents are the sole responsibility of the authors at the University of Oulu, and do not necessarily reflect the views of the European Union or the participating countries.

References

435 Chen, Y., Feng, Q., Zhang, G., Ou, L., Lu, Y., 2007. Study on the recycling of valuable metals in
436 spent Al2O3-based catalyst. Miner. Metall. Process. 24, 30–34.
437 https://doi.org/10.1007/bf03403355

438 Chmielewski, A.G., Urbański, T.S., Migdał, W., 1997. Separation technologies for metals recovery
439 from industrial wastes. Hydrometallurgy 45, 333–344. https://doi.org/10.1016/s0304-
440 386x(96)00090-4

441 Curelaru, I.M., Strid, K.G., Suoninen, E., Minni, E., Rönnhult, T., 1981. Electron structure of excited
442 configurations in Ca2V2O7 studied by electron-induced core-ionization loss spectroscopy,
443 appearance-potential spectroscopy, and x-ray-photoelectron spectroscopy. Phys. Rev. B 23,
444 3700–3709. https://doi.org/10.1103/PhysRevB.23.3700

445 Ding, R., Liu, G., 2011. Advances of Extraction of Vanadium from Solution [J]. Hunan Nonferrous
446 Met. 3.

447 Dupin, J.C., Gonbeau, D., Vinatier, P., Levasseur, A., 2000. Systematic XPS studies of metal oxides,
448 hydroxides and peroxides. Phys. Chem. Chem. Phys. 2, 1319–1324.
449 https://doi.org/10.1039/a908800h

450 Eighmy, T.T., Kinner, A.E., Shaw, E.L., Francis, C.A., 2000. Characterization by XPS : An
451 Environmentally Important Secondary Mineral 6, 193–201.

452 Gomes, H.I., Jones, A., Rogerson, M., Greenway, G.M., Lisbona, D.F., Burke, I.T., Mayes, W.M.,
453 2017. Removal and recovery of vanadium from alkaline steel slag leachates with anion exchange
454 resins. J. Environ. Manage. 187, 384–392. https://doi.org/10.1016/j.jenvman.2016.10.063

455 Guzmán, J., Saucedo, I., Navarro, R., Revilla, J., Guibal, E., 2002. Vanadium interactions with
456 chitosan: Influence of polymer protonation and metal speciation. Langmuir 18, 1567–1573.
457 https://doi.org/10.1021/la010802n

458 Han, C., Li, L., Yang, H., Xue, X.-X., 2018. Preparation of V 2 O 5 from converter slag containing

vanadium. Rare Met. 37, 904–912.

Heuer, J.K., Stubbins, J.F., 1999. An XPS characterization of FeCO3 films from CO2 corrosion. Corros. Sci. 41, 1231–1243.

Hryha, E., Rutqvist, E., Nyborg, L., 2012. Stoichiometric vanadium oxides studied by XPS. Surf. Interface Anal. 44, 1022–1025. https://doi.org/10.1002/sia.3844

Khalid, M.K., Leiviskä, T., Tanskanen, J., 2017. Properties of vanadium-loaded iron sorbent after alkali regeneration. Water Sci. Technol. 76, 2672–2679.

Lazaridis, N.K., Jekel, M., Zouboulis, A.I., 2003. Removal of Cr(VI), Mo(VI), and V(V) ions from single metal aqueous solutions by sorption or nanofiltration. Sep. Sci. Technol. 38, 2201–2219. https://doi.org/10.1081/SS-120021620

Leiviskä, T., 2021. Vanadium (V) removal from water by sorption, in: Sorbents Materials for Controlling Environmental Pollution. Elsevier, pp. 543–571.

Leiviskä, T., Khalid, M.K., Sarpola, A., Tanskanen, J., 2017. Removal of vanadium from industrial wastewater using iron sorbents in batch and continuous flow pilot systems. J. Environ. Manage. 190, 231–242. https://doi.org/10.1016/j.jenvman.2016.12.063

Leiviskä, T., Leskelä, T., Tanskanen, J., 2019. Effect of alkali regeneration on pore characteristics and performance of ferric oxyhydroxide and akaganéite sorbents. J. Water Process Eng. 31, 100838. https://doi.org/10.1016/j.jwpe.2019.100838

Li, G.C., 2011. Determination of the vanadium in aqueous solution by phosphoric acid–sodium tungstate spectrophotometry method. J. Shanxi Coal Manag. Cadre Inst. 24, 141–143.

Li, H., Liu, X., He, H., 2014. Thermodynamic study on vanadium precipitation with calcium salt. Rare Met. Cem. carbides 42, 15–19.

Luo, L., Miyazaki, T., Shibayama, A., Yen, W., Fujita, T., 2003. A novel process for recovery of

tungsten and vanadium from a leach solution of tungsten alloy scrap. Miner. Eng. 16, 665–670. https://doi.org/10.1016/S0892-6875(03)00103-1

Mazurek, K., 2013. Recovery of vanadium, potassium and iron from a spent vanadium catalyst by oxalic acid solution leaching, precipitation and ion exchange processes. Hydrometallurgy 134–135, 26–31. https://doi.org/10.1016/j.hydromet.2013.01.011

Moskalyk, R.R., Alfantazi, A.M., 2003. Processing of vanadium: A review. Miner. Eng. 16, 793–805. https://doi.org/10.1016/S0892-6875(03)00213-9

Muthukumar, K., Patel, K.M., Mohapatra, D., Padh, B., Reddy, B.R., 2020. Selective recovery of vanadium as AMV from calcium vanadate sludge by direct AS leaching process: An industrial approach. Waste Manag. 102, 815–822. https://doi.org/10.1016/j.wasman.2019.11.040

Naeem, A., Westerhoff, P., Mustafa, S., 2007. Vanadium removal by metal (hydr)oxide adsorbents. Water Res. 41, 1596–1602. https://doi.org/10.1016/j.watres.2007.01.002

Navarro, R., Guzman, J., Saucedo, I., Revilla, J., Guibal, E., 2007. Vanadium recovery from oil fly ash by leaching, precipitation and solvent extraction processes. Waste Manag. 27, 425–438. https://doi.org/10.1016/j.wasman.2006.02.002

Ni, M., Ratner, B.D., 2008. Differentiating calcium carbonate polymorphs by surface analysis techniques - An XPS and TOF-SIMS study. Surf. Interface Anal. 40, 1356–1361. https://doi.org/10.1002/sia.2904

Nikiforova, A., Kozhura, O., Pasenko, O., 2017. Application of lime in two-stage purification of leaching solution of spent vanadium catalysts for sulfuric acid production. Hydrometallurgy 172, 51–59. https://doi.org/10.1016/j.hydromet.2017.06.020

Peacock, C.L., Sherman, D.M., 2004. Vanadium(V) adsorption onto goethite (α-FeOOH) at pH 1.5 to 12: A surface complexation model based on ab initio molecular geometries and EXAFS spectroscopy. Geochim. Cosmochim. Acta 68, 1723–1733.

https://doi.org/10.1016/j.gca.2003.10.018

Perron, L., 2001. Vanadium. Nat. Resour. Canada, Miner. Resour. Sect. Canada Miner. Yearb. pp 51–59.

Shao, Y., Feng, Q., Chen, Y., Ou, L., Zhang, G., Lu, Y., 2009. Studies on recovery of vanadium from desilication residue obtained from processing of a spent catalyst. Hydrometallurgy 96, 166–170. https://doi.org/10.1016/j.hydromet.2008.10.005

Silversmit, G., Depla, D., Poelman, H., Marin, G.B., De Gryse, R., 2004. Determination of the V2p XPS binding energies for different vanadium oxidation states (V5+ to V0+). J. Electron Spectros. Relat. Phenomena 135, 167–175. https://doi.org/10.1016/j.elspec.2004.03.004

Sun, Y., Ding, X., Zheng, Z., Cheng, X., Hu, X., Peng, Y., 2006. Magnetic separation of polymer hybrid iron oxide nanoparticles triggered by temperature. Chem. Commun. 2765–2767. https://doi.org/10.1039/b604202c

Vitolo, S., Seggiani, M., Falaschi, F., 2001. Recovery of vanadium from a previously burned heavy oil fly ash. Hydrometallurgy 62, 145–150. https://doi.org/10.1016/S0304-386X(01)00193-1

Vitolo, S., Seggiani, M., Filippi, S., Brocchini, C., 2000. Recovery of vanadium from heavy oil and Orimulsion fly ashes. Hydrometallurgy 57, 141–149. https://doi.org/10.1016/S0304-386X(00)00099-2

Wang, D., Sañudo Wilhelmy, S.A., 2009. Vanadium speciation and cycling in coastal waters. Mar. Chem. 117, 52–58. https://doi.org/10.1016/j.marchem.2009.06.001

Wang, S., Du, H., Zheng, S., Liu, B., Yan, H., Zhang, Y., 2017. New technology from sodium vanadate to vanadium oxide by calcification and carbonization-ammonium process. CIESC J. 68, 2781–2789.

White, D.J., Levy, L.S., 2021. Vanadium: Environmental hazard or environmental opportunity? A

perspective on some key research needs. Environ. Sci. Process. Impacts 23, 527–534. https://doi.org/10.1039/d0em00470g

Yanan, S., Xing, X., Yue, Q., Gao, B., Li, Y., 2020. Nitrogen-doped carbon nanotubes encapsulating Fe/Zn nanoparticles as a persulfate activator for sulfamethoxazole degradation: Role of encapsulated bimetallic nanoparticles and nonradical reaction. Environ. Sci. Nano 7, 1444–1453. https://doi.org/10.1039/d0en00050g

Zhang, D., Ma, Y., Feng, H., Wang, Y., Hao, Y., 2012. Preparation and characterization of the carbon–Microsilica composite sorbent. Adv. Powder Technol. 23, 215–219.

Zhang, R., Lu, J., Dopson, M., Leiviskä, T., 2021a. Vanadium removal from mining ditch water using commercial iron products and ferric groundwater treatment residual-based materials. Chemosphere 286, 131817. https://doi.org/10.1016/j.chemosphere.2021.131817

Zhang, R., Walder, I., Leiviskä, T., 2021b. Pilot-scale field study for vanadium removal from mining-influenced waters using an iron-based sorbent. J. Hazard. Mater. 416. https://doi.org/10.1016/j.jhazmat.2021.125961

Zhang, Y.M., Bao, S.X., Liu, T., Chen, T.J., Huang, J., 2011. The technology of extracting vanadium from stone coal in China: History, current status and future prospects. Hydrometallurgy 109, 116–124. https://doi.org/10.1016/j.hydromet.2011.06.002

Zhao, Z., Long, H., Li, X., Fan, Y., Han, Z., 2012. Precipitation of vanadium from Bayer liquor with lime. Hydrometallurgy 115–116, 52–56. https://doi.org/10.1016/j.hydromet.2011.12.001